SVN Stroke & Vascular Neurology

Deep white matter hyperintensity is spatially correlated to MRI-visible perivascular spaces in cerebral small vessel disease on 7 Tesla MRI

Yajing Huo ,[1] Yilin Wang,[2] Cen Guo ,[1] Qianyun Liu,[1] Lili Shan,[1] Mingyuan Liu,[1] Haibo Wu,[1] Guanwu Li,[3] Huihui Lv,[1] Lingdan Lu,[1] Yintin Zhou,[1] Jianfeng Feng,[4] Yan Han[1]

To cite: Huo Y, Wang Y, Guo C, *et al*. Deep white matter hyperintensity is spatially correlated to MRI-visible perivascular spaces in cerebral small vessel disease on 7 Tesla MRI. *Stroke & Vascular Neurology* 2022;**0**. doi:10.1136/svn-2022-001611

YH and YW contributed equally.
JF and YH contributed equally.

Received 29 March 2022
Accepted 14 September 2022

[1]Department of Neurology, Yueyang Hospital of Integrated Traditional Chinese and Western Medicine, Shanghai University of Traditional Chinese Medicine, Shanghai, China
[2]Georgetown Preparatory School, North Bethesda, Maryland, USA
[3]Department of Radiology, Yueyang Hospital of Integrated Traditional Chinese and Western Medicine, Shanghai University of Traditional Chinese Medicine, Shanghai, China
[4]Institute of Science and Technology for Brain-inspired Intelligence, Fudan University, Shanghai, China

Correspondence to
Dr Yan Han;
hanyan.2006@aliyun.com

ABSTRACT

Background The association between perivascular space (PVS) and white matter hyperintensity (WMH) has been unclear. Normal-appearing white matter (NAWM) around WMH is also found correlated with the development of focal WMH. This study aims to investigate the topological connections among PVS, deep WMH (dWMH) and NAWM around WMH using 7 Tesla (7T) MRI.

Methods Thirty-two patients with non-confluent WMHs and 16 subjects without WMHs were recruited from our department and clinic. We compared the PVS burden between patients with and without WMHs using a 5-point scale. Then, the dilatation and the number of PVS within a radius of 1 cm around each dWMH were compared with those of a reference site (without WMH) in the contralateral hemisphere. In this study, we define NAWM as an area within the radius of 1 cm around each dWMH. Furthermore, we assessed the spatial relationship between dWMH and PVS.

Results Higher PVS scores in the centrum semiovale were found in patients with >5 dWMHs (median 3) than subjects without dWMH (median 2, p = 0.014). We found there was a greater dilatation and a higher number of PVS in NAWM around dWMH than at the reference sites (p<0.001, p<0.001). In addition, 79.59% of the dWMHs were spatially connected with PVS.

Conclusion dWMH, NAWM surrounding WMH and MRI-visible PVS are spatially correlated in the early stage of cerebral small vessel disease. Future study of WMH and NAWM should not overlook MRI-visible PVS.

INTRODUCTION

White matter hyperintensity (WMH), which has been frequently observed in older people, is one radiological feature of cerebral small vessel disease (CSVD).[1] WMH is associated with cognitive impairment,[2] mood disturbances,[3] and gait dysfunction.[4] Punctate WMHs are more diffusely distributed in supratentorial white matter, especially in frontoparietal white matter,[5] while early confluent WMHs are more frequently found in watershed regions.[6] However, the pathogenesis of WMH is yet to be fully understood.[7]

Previous studies have shown that microstructural integrity impairment of the normal-appearing white matter (NAWM) was associated with the development of focal WMH and could continuously aggravate into WMH over time,[8 9] It indicates that NAWM surrounding WMH is associated with impaired structural integrity.[10 11] A further study showed that reduced cerebral blood flow (CBF) and increased blood–brain barrier (BBB) permeability, both of which would increase the likelihood of developing WMH, appeared in the NAWM surrounding WMH.[12]

Perivascular space (PVS) is a fluid-filled chamber revolving around the small vessel in the brain, and it acts as a conduit for fluid transport and clearance of waste proteins.[13] There is accumulating epidemiological evidence suggesting that PVS dilatation is associated with increased severity of WMH.[14 15] Neuropathologically, WMH revealed dilated PVS, demyelination, axonal loss and gliosis.[16] A previous study suggested greater fluid-like properties in NAWM.[17] As PVS correlated with unincorporated anisotropic water, it would be beneficial to study whether PVS changes in the NAWM.[18]

The PVS, being very small, was usually visualised by conventional clinical 1.5 or 3 Tesla MRI sequences. As 7T MRI can provide a higher signal-to-noise ratio (SNR) and spatial resolution of the image, this can offer multiple novel insights into vascular and brain parenchymal damages associated with CSVD, such as better detection of MRI-visible PVS, cerebral microbleeds and microinfarct as well as better vessel wall imaging.[19 20] With 7T MRI, the PVS could be visualised by high-resolution 3D imaging. In this way, smaller PVS and minor morphological changes of the PVS can be more readily detected in a 3D space compared with 3.0T or 1.5T MRI, which

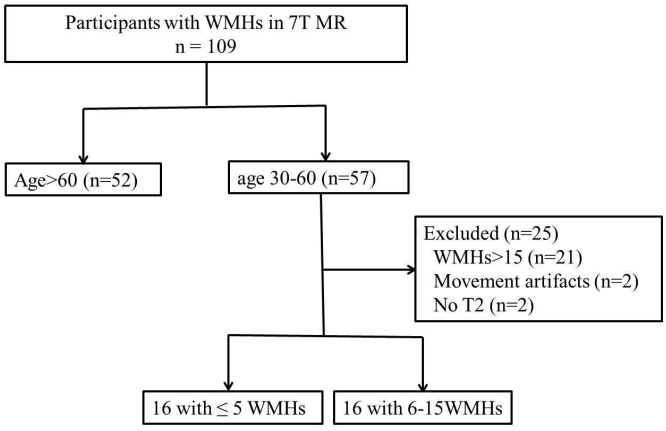

Figure 1 Flow chart of enrollment in this study. WMH, white matter hyperintensity.

may be beneficial to the study of PVS. The purpose of this study is to describe the topological relationship among deep WMH (dWMH), NAWM surrounding WMH, and PVS, with the hypothesis that both dWMH and NAWM would be associated with MRI-visible PVS in patients with CSVD.

METHODS

Participants

The data of consecutive subjects recruited in a prospective longitudinal 7T MRI study between December 2020 and January 2022 from our clinic and department was retrospectively reviewed. This prospective longitudinal 7T MRI study is a single-centre prospective observational study that recruits subjects (age >30) with CSVD. Neuropsychological test, gait analysis and multimodal 7T MRI scan were performed for evaluation of CSVD. Currently the cohort comprises 109 participants. The initial reasons for patients to undergo a diagnostic 3T MRI are mainly comprised, e.g. headache, dizziness, sleep disorders, gait disturbances or memory loss. The inclusion criterion was the presence of CSVD imaging markers (WMHs, or at least one lacuna, or one cerebral microbleed). Exclusion criteria were: (1) secondary WMH, such as immunological, infectious, toxic, metabolic and other causes; (2) abnormal brain lesions, such as brain trauma, intracerebral haemorrhage, non-lacunar cerebral infarction and other intracranial space occupying lesions; (3) MR angiography showing severe intracerebral atherosclerotic stenosis; (4) contra-indications for 7T MRI. All subjects have signed informed consent.

For the current study, we aim to observe the spatial relationship between dWMH, NAWM and PVS in the early stage of CSVD. So we included patients in this prospective longitudinal 7T MRI study who also met the additional inclusion criteria: (1) age 30–60 years; (2) no more than fifteen non-confluent white matter lesions (WMLs) that are larger than 2 mm. The study initially recruited 57 individuals aged 30–60 years. In those, 21 subjects having>15 WMHs, 2 subjects whose images were greatly influenced by movement artefacts and two missing T2 sequences were excluded. Seventeen subjects without WMH/lacuna/cerebral microbleed were also recruited from our department and the clinic as well who also underwent 7T MRI scanning. Of those, one was excluded due to movement artefacts. Finally, 48 participants were involved in the analysis, and 32 of which showed WMHs and 16 did not. Among the 32 participants with WMHs, 16 patients had ≤5 WMLs and 16 patients had >5 WMLs (figure 1).

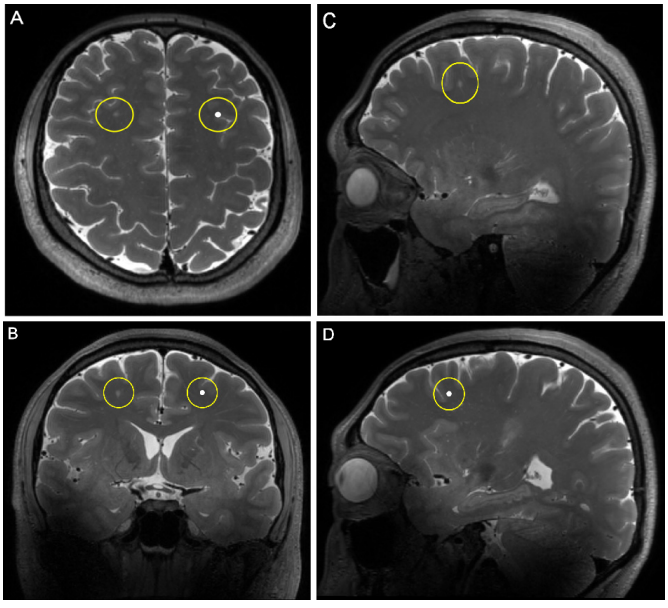

Figure 2 Illustration of reference sites of dWMH. The degrees of the dilatation and number of PVS within a spherical area with a radius of 1 cm around dWMH and the anatomically corresponding reference area in the contralateral hemisphere were evaluated in axil plane (A), coronal plane (B) and sagittal plane (C and D). dWMH, deep white matter hyperintensity; PVS, perivascular space.

MR imaging

All subjects underwent multi-model MRI by 7.0T MRI (MAGNETOM Terra, Siemens Healthcare, Erlangen, Germany) scanner using a 32-channel brain phased array coil. The scanning sequences included: (1) a 3D T2-weighted spcR sequence (voxel size=0.7×0.7×0.7 mm^3, TE/TR=4000/118 ms, flip angle=120°, scan duration 7 min 2 s), used for assessing PVS, (2) a 3D fluid-attenuated inversion recovery (FLAIR) sequence (voxel size=0.7×0.7×0.7 mm^3, TE/TR=9000/270 ms, flip angle=120°, scan duration 4 min 5 s), used for assessing WMH, (3) a T1-weighted sequence with 3D magnetisation-prepared rapid gradient echo (3D-MP2RAGE) (voxel size=0.7×0.7×0.7 mm^3, TE/TI/TR=3800/2.27/2700 ms, scan duration 6 min 37 s), used for mirroring WMHs to the contralateral hemisphere to generate reference sites, (4) a 3D susceptibility weighted imaging (SWI) sequence (pixel size=0.12×0.12 mm, slice thickness=1.5 mm, TE/TR=9.54/21 ms, flip angle=10°, scan duration 6 min 37 s), used for assessing cerebral microbleeds (CMBs). These participants also underwent 3.0T MRI scanner (Philips

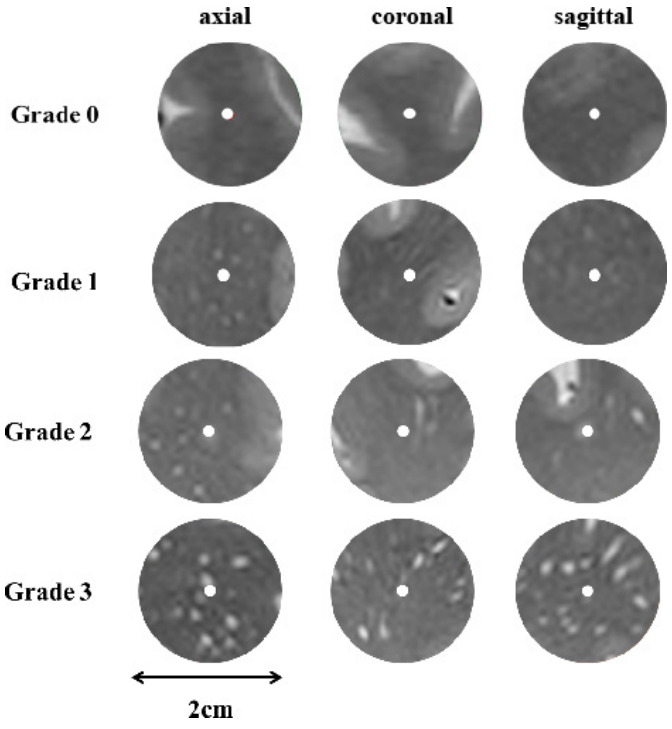

Figure 3 The reference template used for the grading of PVS. From above to below, each template illustrates different extents of the dilatation of PVS. A single location was revealed in three directions (from left to right: axial, coronal, sagittal) in each row. PVS, perivascular space.

Ingenia, Philips Healthcare, Best, Netherlands). The MRI protocol included T1-weighted sequence (TE=2.3 ms, TR=250 ms, flip angle=75°, matrix size=512×512×18, voxel size=0.45 mm×0.45mm×6 mm), T2-weighted FLAIR sequence (TE=120 ms, TR=7000 ms, flip angle=90°, matrix size=384×384×18, voxel size=0.6 mm×0.6mm×6 mm) and time-of-flight MRA (TE=3.5 ms, TR=23 ms, flip angle=18°, matrix size=560×560×112, voxel size=0.375 mm×0.375mm×0.8 mm).

Image analysis

All imaging markers of CSVD were evaluated according to the Standards for Reporting Vascular Changes on Neuroimaging.[21] PVS was defined as a thin linear or small punctate structure of cerebrospinal fluid intensity with a diameter generally<3 mm that ran perpendicular to the brain's surface and were parallel to the perforating vessels. We recognise PVS in axial, sagittal and coronal direction to appreciate the 3D shape of possible PVS.

Rating of PVS in subjects with and without dWMHs

The burden of PVS in the basal ganglia (BG-PVS) and the centrum semiovale (CSO-PVS) were respectively rated on T2 sequences of 7.0T MRI. In BG and CSO, the slice with the maximum number of PVS was used for the rating. In BG and CSO, PVS were rated using a five-point score[22]: Grade 0 for no PVS, Grade 1 for 1–10 PVS, Grade 2 for 11–20 PVS, Grade 3 for 21–40 PVS, Grade 4 for>40 PVS.

Comparison PVS dilatation and number between NAWM surrounding dWMHs and reference sites

The FLAIR images were registered to the T2 images to present the spatial association of NAWM surrounding dWMH and PVS in 7.0T MRI. T2-FLAIR images were registered to the T2-weighted images with an affine transformation based on the statistical parametric mapping 12 registration packages (www.fil.ion.ucl.ac.uk/spm). We assessed the PVS dilatation in a sphere with a radius of 1 cm surrounding dWMH and the symmetrical reference region in the contralateral hemisphere (figure 2). A radius of 1 cm was chosen in this study because microstructural changes were usually reported to extend 2–9 mm from the WMHs.[11] WMH and reference site were blinded to the rater by masking out the sphere's centre (ie, the site of the WMH or the reference site). WMH was ruled out from the analysis if another WMH was located within its reference area. The overall number of WMHs in these subjects was 196 and 32 dWMHs were excluded because dWMHs were also located at the reference sites in the contralateral hemisphere. Finally 164 dWMHs in total were used for the analysis.

We used the four-point rating scale to evaluate the dilatation of PVS[23]: Grade 0 for no PVS, Grade 1 for a few small punctate PVS, Grade 2 for several moderately dilated PVS, Grade 3 for many severely dilated PVS(-figure 3). The degree of PVS dilatation within a 1 cm radius around the selected locations was evaluated in three directions (sagittal, coronal and axial), respectively (figure 2). The PVS score is the highest score of the regions' scores in three directions. The degree of PVS dilatation of 164 dWMHs and 164 reference sites was evaluated by two raters who showed good agreement (intraclass correlation coefficient (ICC)=0.86).

We also counted the number of PVS within 1 cm radius around the selected locations (164 dWMHs and 164 reference sites) in three directions (sagittal, coronal and axial) respectively. The sum of the number of PVS in three directions was calculated. We used a six-point rating scale to evaluate the sum of number of PVS as follows: grade 0 for no PVS, grade 1 for 1–5 PVS, grade 2 for 6–10 PVS, grade 3 for 11–15 PVS, grade 4 for 16–20 PVS, grade 5 for>20 PVS. The grade of the number of PVS was counted by two raters with excellent agreement (ICC=0.90).

Visual assessment of the spatial relationship between dWMHs and PVS

We classified the WMH into three types as previous study: (1) Type 1, topologically connected with a single PVS; (2) Type 2, topologically connected with multiple PVS; (3) Type 3, does not connect to any PVS (figure 4).[24] Two raters blinded to each other assessed the topological association between WMH and PVS. There were 196 dWMHs in these patients. The inter-rater kappa was 0.7.

Statistical analysis

The Wilcoxon-signed rank test was used to compare the PVS scores around WMHs and reference sites. The

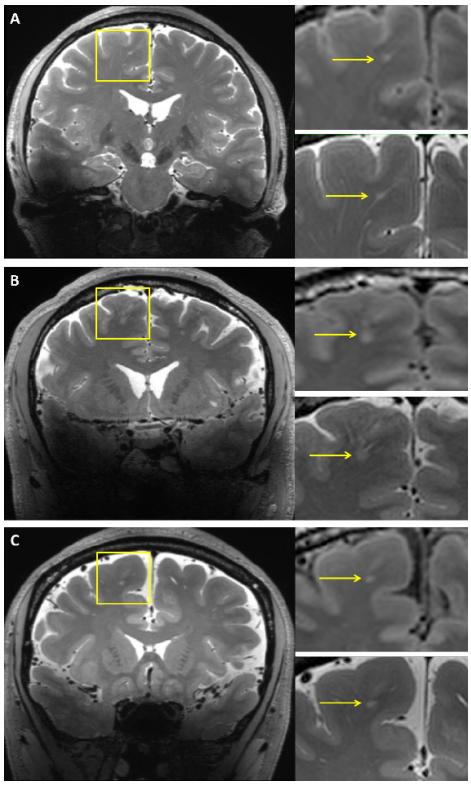

Figure 4 Illustration of spatial connections between WMH and PVS. (A) Type 1, small punctate WMH (yellow arrow) was spatially connected with one PVS tube. (B) Type 2, flake-like WMH (yellow arrow) was connected with multiple tubes. (C) Type 3, insular WMH (yellow arrow) without PVS connection. PVS, perivascular space; WMH, white matter hyperintensity.

Mann-Whitney U test was used to compare the degree of PVS dilatation between subjects with and without WMHs. In table 1, one-way analysis of variance was used to compare age among three groups. Chi square test or Fisher's exact test was applied to compare the difference between categorical variables.

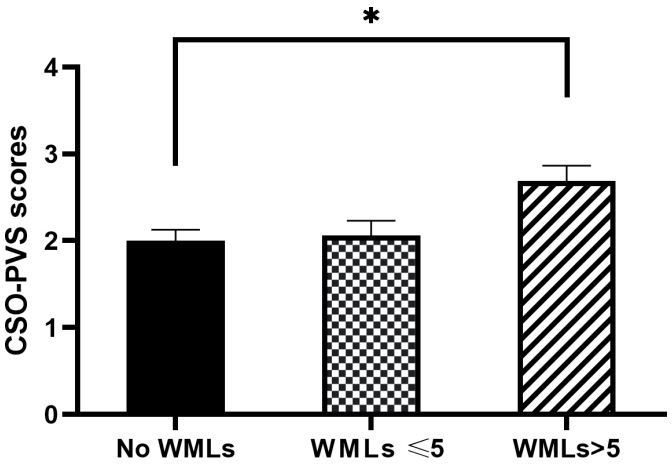

Figure 5 Comparison of CSO-PVS scores among subjects without, with ≤5 and with >5 WMLs. *indicates p<0.05. The results are showed as means±SEM. CSO-PVS, centrum semiovale-perivascular space; WMLs, white matter lesions.

RESULTS

Demographics

Thirty-two patients with WMHs (13 females; Mean age±SD 44.03±6.41 years; range 33–58 years) were enrolled in this study, in which 16 patients had ≤5 WMLs and 16 patients had >5 WMLs. Sixteen subjects without WMHs (6 females; Mean age±SD 42.75±6.26 years; range 33–54 years) were recruited as the control group. Baseline clinical characteristics are presented in table 1. In the patients with WMHs, the total number of WMHs in these subjects was 196.Baseline characteristics were not statistically different among patients with ≤5 WMLs, patients with >5 WMLs and controls without WMLs.

Comparison of burden of PVS between subjects with and without dWMHs

Patients with >5 WMLs (n=16) showed higher CSO-PVS scores (median 3) than subjects (n=16) without WMHs (median 2) (Z=−2.794, p=0.014) (figure 5). No statistically

Table 1 Baseline characteristics of patients with WMHs and controls without WMHs

	Patients with WMHs			
Category	≤5 WMLs (n=16)	>5 WMLs (n=16)	Controls (n=16)	P value
Age (mean±SD, year)	44.06±6.13	44.00±6.89	42.75±6.26	0.81
Female, n (%)	7 (43.8)	6 (37.5)	6 (37.5)	0.917
Current smoker, n (%)	3 (18.8)	3 (18.8)	2 (12.5)	1
Alcohol user, n (%)	0 (0.0)	1 (6.3)	3 (18.8)	0.304
Hypertension, n (%)	1 (6.3)	3 (18.8)	2 (12.5)	0.859
Diabetes mellitus, n (%)	0 (0.0)	0 (0.0)	1 (6.3)	1
Hyperlipidaemia, n (%)	2 (12.5)	5 (31.3)	3 (18.8)	0.556
Lacunes, n(%)	0 (0.0)	3 (18.6)	0 (0.0)	0.097
CMBs, n(%)	1 (6.3)	1 (6.3)	0 (0.0)	1

CMBs, cerebral microbleeds; WMH, white matter hyperintensity; WML, white matter lesion.

significant difference in BG-PVS scores (Z=−1.791, p=0.381) was found between subjects without WMHs and patients with>5 WMLs. No statistically significant difference in CSO-PVS scores (Z=−0.314, p=0.809) and BG-PVS scores (Z=−0.000, p=1.000) were found between subjects without WMHs and patients with ≤5 WMLs.

Comparison of PVS dilatation and number between NAWM surrounding dWMHs and contralateral reference sites

Thirty-two dWMHs were excluded because dWMHs were also present at the contralateral reference sites. Finally a total of 164 dWMHs were used for the analysis. The number of PVS and the degree of PVS dilatation were rated by two raters who showed good consistency (ICC=0.86, ICC=0.90). The degree of PVS dilatation in NAWM around dWMH was higher than that at reference sites in the contralateral hemisphere (Z=−5.488, p<0.001, see table 2). As well, there was a significantly higher degree of PVS number in NAWM around dWMH compared with that at reference sites in the contralateral hemisphere (Z=−7.184, p<0.001, see table 3).

The spatial relationship between dWMHs and PVS

In this study, we observed that some WMHs were spatially connected to PVS. So we further investigated the spatial relationship between dWMHs and PVS. There were 196 dWMHs used for the analysis of the spatial relationship between dWMHs. The two raters showed good consistency (Kappa=0.7). We found 79.59% dWMHs were spatially connected with one or more PVS tubes. In these 196 dWMHs, 143 dWMHs (72.95%) were topologically connected with a single PVS tube, 13 (6.63%) were topologically connected with multiple PVS tubes and 40 dWMHs (20.40%) were not connected to any PVS.

DISCUSSION

In the current study, we found strong topological relationship among dWMH, NAWH around dWMH and PVS in the early stage of CSVD. The PVS burden in centrum semiovale was higher in patients with >5 dWMHs than in subjects without WMH. We also found most punctate dWMH were spatially connected with PVS, and the degree of dilatation and the number of PVS in the NAWM surrounding dWMH were higher than that at reference sites in the contralateral hemisphere.

Previous study has shown association between increased dilated PVS in white matter and DWMH volume.[15] In this 7T MRI study, we also found that the number of dWMHs was related to the burden of PVS in centrum semiovale, but not with the burden of PVS in basal ganglia. Recently, a study found that most deep WMHs were topologically connected with PVS.[24] In our study, we found 79.59% dWMHs were spatially connected with one or multiple PVS tubes in patients with punctuate DWMHs who is in the early stage of CSVD in 7T MRI. These data indicated that PVS were associated with WMHs and the mechanisms underlying the development of MRI-visible PVS may differ in different brain regions.

The increased SNR and spatial resolution of the 7T 3D T2-weighted sequence could discern more PVS.[25] We evaluated the degree of PVS dilatation and the number of PVS around the WMH in three directions (sagittal, coronal and axial) by a four-point rating scale and a six-point rating scale respectively. In practice, we found that the PVS number differs in three directions. Then we defined the PVS count score as the sum of the PVS number in

Table 2 The degree of PVS dilatation in NAWM surrounding dWMH and reference site

	Reference site			
N(%)	0	1	2	Total
dWMH				
0	0 (0.0%)	2 (100%)	0 (0.0%)	2
1	3 (3.2%)	85 (91.4%)	5 (5.4%)	93
2	3 (4.5%)	39 (59.1%)	24 (36.4%)	66
3	0 (0.0%)	1 (33.3%)	2 (66.7%)	3
total	6	127	31	164

dWMH, deep white matter hyperintensity; NAWM, normal-appearing white matter; PVS, perivascular space.

Table 3 The degree of PVS number in NAWM surrounding dWMH and reference site

	Reference site						
N (%)	0	1	2	3	4	5	Total
dWMH							
0	0 (0.0%)	2 (100%)	0 (0.0%)	0 (0.0%)	0 (0.0%)	0 (0.0%)	2
1	5 (8.9%)	48 (85.7%)	3 (5.4%)	0 (0.0%)	0 (0.0%)	0 (0.0%)	56
2	1 (1.4%)	40 (55.6%)	27 (37.5%)	4 (5.6%)	0 (0.0%)	0 (0.0%)	72
3	0 (0.0%)	7 (30.4%)	14 (60.9%)	2 (8.7%)	0 (0.0%)	0 (0.0%)	23
4	0 (0.0%)	2 (25.0%)	2 (25.0%)	4 (50.0%)	0 (0.0%)	0 (0.0%)	8
5	0 (0.0%)	0 (0.0%)	1 (33.3%)	0 (0.0%)	1 (33.3%)	1 (33.3%)	3
Total	6	99	47	10	1	1	164

dWMH, deep white matter hyperintensity; NAWM, normal-appearing white matter; PVS, perivascular space.

three directions to reflect the overall load of PVS around a certain WMH. Moreover, we minimised the confounding by comparing WMH to a reference site within the same individual, as the number and morphology of PVS might differ in different individuals. And we found the degree of PVS dilatation and the number of PVS in the NAWM surrounding dWMH was higher than that at reference sites in the contralateral hemisphere.

Previous studies have suggested that decreased CBF and BBB disruption participated in the pathogenesis of WMH and NAWM closer to the WMH.[12 26–28] In a study using rodent models, early BBB breakdown can result in a significant increase in the number of dilated PVS in the white matter, suggesting that BBB breakdown can result in increased fluid in the PVS.[29] In the human study, impaired BBB was also associated with the number of enlarged PVS.[30] As BBB disruption might involve in the pathogenesis of WMH, NAWM and dilated PVS, we speculate that dilated PVS in the NAWM surrounding WMH might be due to the increased blood-brain-barrier leakage. The serum protein extravasation can accumulate in the perivascular tissues due to BBB disruption, which might result in less clearance of waste proteins from the interstitial fluid space.[31 32] The dilated PVS may play a role in the vicious cycle in BBB disruption and ultimately impaired the waste proteins clearance from the interstitial fluid space, resulting in accumulation of toxins and tissue damage, finally leading to the formation of WMH.[31]

However, our study also has limitations. First, this study is an explorative study, and the sample size was comparatively small, while the number of WMHs in our population was still substantial. Second, we did not quantitatively assess the diameter and volume of PVS. Thirdly, we didn't quantify the BBB disruption in WMH and NAWM surrounding WMH. Previous studies have demonstrated that BBB disruption participated in the pathogenesis of WMH and NAWM closer to the WMH.[12 26 28] In the future study, measurements of the BBB disruption in WMH and NAWM would be useful to further investigate the relationship between MRI-visible PVS and NAWM surrounding WMH.

CONCLUSION

In conclusion, we found a topographical association among dWMH, NAWM surrounding WMH, and MRI-visible PVS. This may broaden our insight in the pathophysiology underlying WMH and NAWM surrounding WMH. Further investigation into NAWM surrounding WMH in CSVD should consider the role of MRI-visible PVS and dynamically follow-up the spatial relationships of dWMH, NAWM surrounding WMH and MRI-visible PVS.

Contributors YH: study concept and design, drafted and revised the manuscript, statistical analysis, data acquisition and interpretation, MRI processing. YW: study concept and design, drafted and revised the manuscript, data acquisition, MRI processing. CG: data acquisition, MRI processing. QL: data acquisition, MRI processing. LS: data acquisition, MRI processing. ML: study supervision and coordination, data acquisition. HW: study supervision and coordination, data acquisition. GL: study supervision and coordination, data acquisition. HL: data acquisition, MRI processing. LL: data acquisition, MRI processing. YZ: data acquisition, MRI processing. JF: study concept and design, study supervision and coordination, revised the manuscript. YH: acted as the guarantor who accepted full responsibility for the work, had access to the data, and controlled the decision to publish, study concept and design, study supervision and coordination.

Funding The authors disclosed receipt of the following financial support for the research, authorship, and/or publication of this article: This study was funded by the National Key Research and Development Project (NO. 2019YFC1711600, 2019YFC1711603), National Natural Science Foundation of China (No.81771288) and Clinical Research Plan of Shanghai Hospital Development Center (No. SHDC2020CR2046B).

Competing interests None declared.

Patient consent for publication Not applicable.

Ethics approval This study involves human participants and was approved by the Ethics Committee of Yueyang Hospital of Integrated Traditional Chinese and Western Medicine, Shanghai University of Tranditional Chinese Medicice (2020-060). Participants gave informed consent to participate in the study before taking part.

Provenance and peer review Not commissioned; externally peer reviewed.

Data availability statement Data are available on reasonable request.

ORCID iDs
Yajing Huo http://orcid.org/0000-0001-6953-8173
Cen Guo http://orcid.org/0000-0002-6845-0476

REFERENCES

1 Shi Y, Wardlaw JM. Update on cerebral small vessel disease: a dynamic whole-brain disease. *Stroke Vasc Neurol* 2016;1:83–92.
2 de Havenon A, Sheth KN, Yeatts SD, *et al*. White matter hyperintensity progression is associated with incident probable dementia or mild cognitive impairment. *Stroke Vasc Neurol* 2022;0:1–3.
3 van Uden IWM, Tuladhar AM, de Laat KF, *et al*. White matter integrity and depressive symptoms in cerebral small vessel disease: the run DMC study. *Am J Geriatr Psychiatry* 2015;23:525–35.
4 Kim YJ, Kwon HK, Lee JM, *et al*. Gray and white matter changes linking cerebral small vessel disease to gait disturbances. *Neurology* 2016;86:1199–207.
5 Medrano Martorell S, Cuadrado Blázquez M, García Figueredo D, *et al*. [Hyperintense punctiform images in the white matter: a diagnostic approach]. *Radiologia* 2012;54:321–35.
6 Enzinger C, Smith S, Fazekas F, *et al*. Lesion probability maps of white matter hyperintensities in elderly individuals: results of the Austrian stroke prevention study. *J Neurol* 2006;253:1064–70.
7 Wardlaw JM, Smith C, Dichgans M. Small vessel disease: mechanisms and clinical implications. *Lancet Neurol* 2019;18:684–96.
8 van Leijsen EMC, Bergkamp MI, van Uden IWM, *et al*. Progression of white matter hyperintensities preceded by heterogeneous decline of microstructural integrity. *Stroke* 2018;49:1386–93.
9 Promjunyakul N-O, Dodge HH, Lahna D, *et al*. Baseline NAWM structural integrity and CBF predict periventricular WMH expansion over time. *Neurology* 2018;90:e2119–26.
10 Wharton SB, Simpson JE, Brayne C, *et al*. Age-associated white matter lesions: the MRC cognitive function and ageing study. *Brain Pathol* 2015;25:35–43.
11 Promjunyakul N-O, Lahna DL, Kaye JA, *et al*. Comparison of cerebral blood flow and structural penumbras in relation to white matter hyperintensities: a multi-modal magnetic resonance imaging study. *J Cereb Blood Flow Metab* 2016;36:1528–36.
12 Wong SM, Jansen JFA, Zhang CE, *et al*. Blood-brain barrier impairment and hypoperfusion are linked in cerebral small vessel disease. *Neurology* 2019;92:e1669–77.
13 Wardlaw JM, Benveniste H, Nedergaard M, *et al*. Perivascular spaces in the brain: anatomy, physiology and pathology. *Nat Rev Neurol* 2020;16:137–53.

14 Doubal FN, MacLullich AMJ, Ferguson KJ, *et al*. Enlarged perivascular spaces on MRI are a feature of cerebral small vessel disease. *Stroke* 2010;41:450–4.
15 Zhu Y-C, Tzourio C, Soumaré A, *et al*. Severity of dilated Virchow-Robin spaces is associated with age, blood pressure, and MRI markers of small vessel disease: a population-based study. *Stroke* 2010;41:2483–90.
16 Grafton ST, Sumi SM, Stimac GK, *et al*. Comparison of postmortem magnetic resonance imaging and neuropathologic findings in the cerebral white matter. *Arch Neurol* 1991;48:293–8.
17 Khan W, Khlif MS, Mito R, *et al*. Investigating the microstructural properties of normal-appearing white matter (NAWM) preceding conversion to white matter hyperintensities (WMHs) in stroke survivors. *Neuroimage* 2021;232:117839.
18 Sepehrband F, Cabeen RP, Choupan J, *et al*. Perivascular space fluid contributes to diffusion tensor imaging changes in white matter. *Neuroimage* 2019;197:243–54.
19 Cannistraro RJ, Badi M, Eidelman BH, *et al*. CNS small vessel disease: a clinical review. *Neurology* 2019;92:1146–56.
20 Benjamin P, Viessmann O, MacKinnon AD, *et al*. 7 Tesla MRI in cerebral small vessel disease. *Int J Stroke* 2015;10:659–64.
21 Wardlaw JM, Smith EE, Biessels GJ, *et al*. Neuroimaging standards for research into small vessel disease and its contribution to ageing and neurodegeneration. *Lancet Neurol* 2013;12:822–38.
22 Potter GM, Chappell FM, Morris Z, *et al*. Cerebral perivascular spaces visible on magnetic resonance imaging: development of a qualitative rating scale and its observer reliability. *Cerebrovasc Dis* 2015;39:224–31.
23 Bouvy WH, van Veluw SJ, Kuijf HJ, *et al*. Microbleeds colocalize with enlarged juxtacortical perivascular spaces in amnestic mild cognitive impairment and early Alzheimer's disease: a 7 Tesla MRI study. *J Cereb Blood Flow Metab* 2020;40:739–46.
24 Huang P, Zhang R, Jiaerken Y, *et al*. Deep white matter hyperintensity is associated with the dilation of perivascular space. *J Cereb Blood Flow Metab* 2021;41:2370–80.
25 Bouvy WH, Biessels GJ, Kuijf HJ, *et al*. Visualization of perivascular spaces and perforating arteries with 7 T magnetic resonance imaging. *Invest Radiol* 2014;49:307–13.
26 Wardlaw JM, Makin SJ, Valdés Hernández MC, *et al*. Blood-brain barrier failure as a core mechanism in cerebral small vessel disease and dementia: evidence from a cohort study. *Alzheimer's & Dementia* 2017;13:634–43.
27 Shi Y, Thrippleton MJ, Makin SD, *et al*. Cerebral blood flow in small vessel disease: a systematic review and meta-analysis. *J Cereb Blood Flow Metab* 2016;36:1653–67.
28 Walsh J, Tozer DJ, Sari H, *et al*. Microglial activation and blood-brain barrier permeability in cerebral small vessel disease. *Brain* 2021;144:1361–71.
29 Montagne A, Nikolakopoulou AM, Zhao Z, *et al*. Pericyte degeneration causes white matter dysfunction in the mouse central nervous system. *Nat Med* 2018;24:326–37.
30 Wardlaw JM, Doubal F, Armitage P, *et al*. Lacunar stroke is associated with diffuse blood-brain barrier dysfunction. *Ann Neurol* 2009;65:194–202.
31 Brown R, Benveniste H, Black SE, *et al*. Understanding the role of the perivascular space in cerebral small vessel disease. *Cardiovasc Res* 2018;114:1462–73.
32 Benveniste H, Liu X, Koundal S, *et al*. The Glymphatic system and waste clearance with brain aging: a review. *Gerontology* 2019;65:106–19.